Bioorganic & Medicinal Chemistry 17 (2009) 1681–1692

Contents lists available at ScienceDirect

Bioorganic & Medicinal Chemistry

journal homepage: www.elsevier.com/locate/bmc

1-Malonyl-1,4-dihydropyridine as a novel carrier for specific delivery of drugs to the brain

Heba A. Hassan [a], Mohamed Abdel-Aziz [a,*], Gamal El-Din A. A. Abuo-Rahma [a], Hassan H. Farag [b]

[a] Department of Medicinal Chemistry, Faculty of Pharmacy, Minia University, 61519-Minia, Egypt
[b] Department of Pharmaceutical Medicinal Chemistry, Faculty of Pharmacy, Assiut University, 71526-Assiut, Egypt

ARTICLE INFO

Article history:
Received 28 September 2008
Revised 17 December 2008
Accepted 22 December 2008
Available online 29 December 2008

Keywords:
1,4-Dihydropyridine
CDS
INH
Malonic acid
Antidepressant

ABSTRACT

A group of 1-malonyl-1,4-dihydropyridine derivatives were synthesized as novel carrier systems for site-specific and sustained drug delivery to the brain. Such carriers are expected to be stable against air oxidation due to the presence of the carbonyl group close to nitrogen of the dihydropyridine. These carrier systems were attached to a group of different aldehydes to afford novel quaternary pyridinium derivatives **9a–e**, **11a–d**, **13** and **18a–b**. Reduction of the prepared quaternary pyridinium derivatives with sodium dithionite afforded a novel group of 1-malonyl-1,4-dihydropyridine chemical delivery systems (CDSs) **10a–e**, **12a–d**, **14** and **19a–b**. The synthesized 1-malonyl-1,4-dihydropyridine CDSs were subjected to various chemical and biological investigations to evaluate their ability to cross the blood–brain barrier, and to be oxidized biologically into their corresponding quaternary derivatives. The in vitro oxidation studies showed that most of the 1-malonyl-1,4-dihydropyridine CDSs could be oxidized into their corresponding quaternary derivatives at an adequate rate. The in vivo studies showed that compounds **10c** and **14** were able to cross the blood–brain barrier at detectable concentrations. Moreover, the pyridinium quaternary intermediates **9a**, **9c**, **13**, **18a** and their corresponding dihydro derivatives **10a**, **10c**, **14** and **19a** were screened for their antidepressant activity using tail suspension behavioral despair test compared to imipramine as a reference at a dose level of 10 mg/kg. The results indicated that compounds **13**, **14** and **19a** induced remarkable antidepressant activity comparable to imipramine. Compounds **10a**, **10c** and **18a** exhibited good antidepressant activity, their activities nearly equal to 92.8%, 86.7% and 90.20% of the activity of imipramine, respectively. The other derivatives **9a** and **9c** exhibited moderate antidepressant activity compared with imipramine.

1. Introduction

The blood–brain barrier is a major impediment for the treatment of central nervous system diseases. Since many drugs are unable to reach this organ at therapeutic concentrations.[1] Various attempts have been made to overcome the limiting access of drugs to the brain and at the same time, reduce the systemic side effects that are common with general treatments.[2–7] One of these attempts was the linking of the active compound to a brain-specific carrier to give a chemical delivery system (CDS) which delivers the active compound specifically into the brain after its cleavage from the carrier at the site of action.[8–13]

The dihydropyridine↔pyridinium salt redox system was described as a general and flexible method for site-specific and sustained delivery of drugs to the brain.[14,15] The biologically active compound linked to a lipoidal dihydropyridine carrier easily penetrates the blood–brain barrier; oxidation of the carrier moiety in vivo to the ionic pyridinium salt prevents its elimination from the brain (locked-in), while elimination from the general circulation is accelerated. By time, the drug is released from the carrier in the brain at a rate depending on the connecting group. The main obstacle faced the industrial development of the idea is the very short life time of the compound, mainly due to their fast air oxidation and/or hydration of the 5,6-double bond, which is a common problem with all the 1,4-dihydropyridine↔pyridinium salt redox CDSs.[16,17]

In the present proposal, a novel carrier was investigated keeping in mind all the requirements for a safe and useful brain-specific chemical delivery system including; reasonable shelf life time, a good rate of oxidation, not be neurotoxic and should be excreted from the brain in a reasonable rate. The system will be used to deliver certain drugs specifically to the brain. The suggested carrier is 1-malonyl-1,4-dihydropyridine, such carrier is expected to be stable against air oxidation due to the presence of the carbonyl group close to nitrogen of the dihydropyridine. Such group will act as electron withdrawing group, whether by resonance or induction, which will result in

* Corresponding author. Tel./fax: +20 86 2369075.
E-mail address: abulnil@hotmail.com (M. Abdel-Aziz).

0968-0896/$ - see front matter © 2008 Elsevier Ltd. All rights reserved.
doi:10.1016/j.bmc.2008.12.051

decreasing the electron density on the ring nitrogen. It is well known that the lone pair of electrons on the ring nitrogen is the initiator of oxidation and/or hydration of the dihydropyridine.[16,17] Accordingly, reduction of the electron density on the ring nitrogen may result in shelf-stable carrier system. On administration, hydrolysis of the ester function follows distribution to give the corresponding 1,4-dihydropyridine-1-malonyl monoanion derivatives at the physiological pH (7.4). The rate of oxidation of the anion is expected to be accelerated, firstly by destabilization of the ground state, secondly by stabilization of the oxidation transition state, and thirdly by stabilization of the final quaternary product. The acid anion function at the vicinity of the nitrogen atom of the dihydro derivatives reduces the energy of the transition state of the enzymatic oxidation to the corresponding quaternary. One of the carboxylic groups of malonic acid may be utilized to connect selected drugs through an amide or ester function, the $CONHNH_2$– group at C_3 or C_4 may be also used to connect a drug moiety (Fig. 1).

Another strategy was designed in this work is the evaluation of the antidepressant activity for some of the novel synthesized dihydro derivatives and their corresponding quaternary derivatives using tail suspension behavioral despair test compared to imipramine as a reference drug at a dose level of 10 mg/kg. The aim is to target the potential antidepressant agents to the brain in order to avoid the serious peripheral side effects associated with their use such as cardiovascular dysfunctions, sexual disturbances, and central nervous system side effects.[18] In the future, the designed 1-malonyl-1,4-dihydropyridine derivatives may be utilized to deliver isonicotinic acid hydrazide (INH) into the brain aiming in treatment of the brain TB in the same time avoiding the systemic side effects associated with the use of INH.

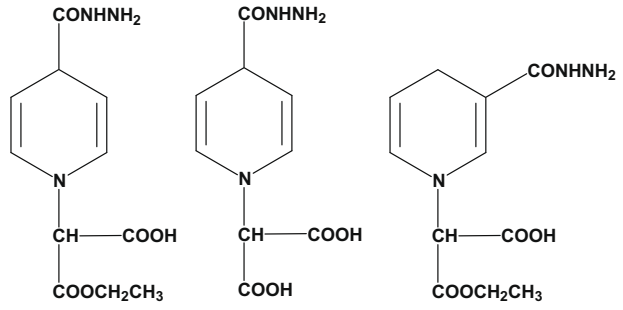

Figure 1. Different forms of the designed 1-malonyl-1,4-dihydropyridine CDS.

2. Results and discussion

2.1. Chemistry

Bromomalonate **3** and bromomalonic acid **5** were prepared according to Scheme 1. Partial hydrolysis of diethylmalonate **1** with alcoholic potassium hydroxide in a ratio of 2:1, respectively, under dry condition followed by acidification of the obtained solution with HCl afforded the corresponding malonic acid monoethyl ester **2** in 40% yield.[19] Treatment of the malonic monoester **2** and malonic acid **4** with Br_2 in glacial acetic acid to afford the corresponding 2-bromomalonic acid monoethyl ester **3** and 2-bromomalonic acid **5** in 60% and 48% yield, respectively.[20,21]

The first group of the designed malonic acid monoethyl ester pyridine chemical delivery systems MEPCDSs 10a-e was successfully synthesized as illustrated in Scheme 2. Heating at reflux of isonicotinic acid hydrazide 6 with different aromatic aldehydes including 2-hydroxybenzaldehyde **7a**[22], 4-methoxybenzaldehyde **7b**[23], 2-chlorobenzaldehyde **7c**[24], 4-hydroxy-3-methoxybenzaldehyde **7d**[25] and 4-(*N*,*N*-dimethylamino)benzaldehyde 7e[26], respectively, in absolute ethanol for 6–8 h to afford the corresponding benzylideneisonicotinic acid hydrazide derivatives **8a–e** in 60–82% yield. The quaternary pyridinium derivatives **9a–e** were prepared by heating at reflux of compounds **8a–e** with 2-bromomalonic acid monoethyl ester **3** in absolute ethanol for 30 h affording **9a–e** in 40–70% yield, Scheme 2. The IR spectra of the prepared compounds **9a–e** showed an absorption band at 1730–1745 cm^{-1}, due to the ν (C=O) stretching of the carboxylic acid moiety and strong absorption band in the region of 1739–1755 cm^{-1} related to the ν (C=O) stretching of the ester moiety. A sharp absorption band at 1668–1682 cm^{-1} due to the ν (C=O) stretching of the amide moiety, in addition to broad bands in the region of 3000–3450 cm^{-1} due to ν (NH) and (OH) stretching. The ^1H NMR spectra recorded for the prepared quaternary compounds **9a–e** showed prominent triplet signal corresponding to the CH_3 protons at δ 1.1–1.3 ppm and quartet signals appear at δ 4.2–4.4 ppm indicating the 2 protons of CH_2. A characteristic downfield shift of the CH protons attached to the nitrogen of pyridinium moiety was observed to appear at δ 5.7–5.9 ppm. The protons belonging to the aromatic system and azomethine were observed at the expected chemical shifts and integral values.

The designed MEPCDSs **10a–e** were prepared in 60–70% yield through reduction of the corresponding quaternary derivatives **9a–e** using sodium dithionite in the presence of sodium bicarbonate in CH_2Cl_2 under atmosphere of nitrogen.[27] Methylene chloride serves to extract the MEPCDSs **10a–e** as soon as it is formed to protect it from degradation in the alkaline aqueous medium.

Another group of *N*-methyl PCDSs **12a–d** and malonyl pyridine chemical delivery system MPCDS **14** were prepared as illustrated

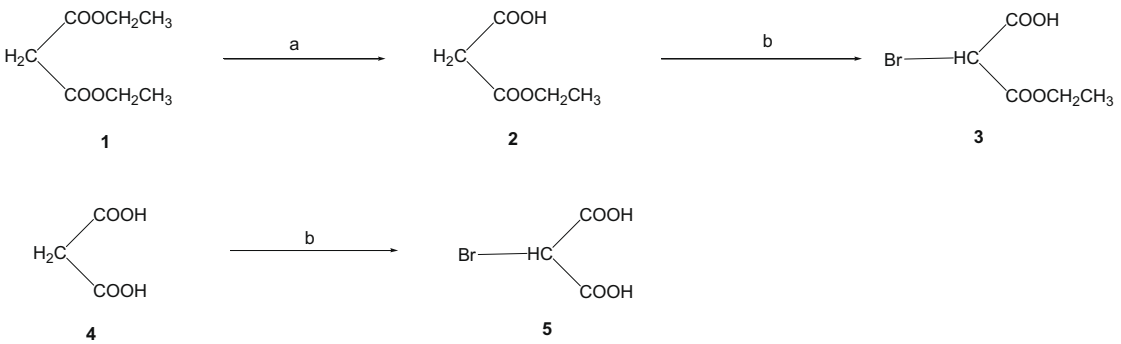

Scheme 1. Synthesis of bromomalonate derivatives **3** and **5**. Reagents: (a) KOH, EtOH, HCl; (b) Br_2, HOAc.

in Scheme 3. Heating at reflux of different Schiff bases **8a–d** with bromomalonic acid **5** in absolute ethanol for about 30 h afforded the corresponding *N*-methyl quaternary pyridinium derivatives **11a–d** in 40–61% yield. In this reaction, quaternization occurs first then followed by decarboxylation. The IR spectra of the prepared compounds **11a–d** showed an absorption bands in the region of 1617–1664 cm^{-1} due to ν (C=O) stretching of the amide moiety. In addition, an absorption bands in the region of 3423–3441cm^{-1} related to ν (NH) stretching. The ^{1}H NMR spectra recorded for the prepared compounds **11a–d** showed a prominent singlet signal at δ 4.4 ppm related to the protons of CH_3 attached to pyridinium nitrogen, the protons belonging to the aromatic system and azomethine were observed at the expected chemical shifts and integral values. Mass spectra and elemental analyses clearly support the proposed structures.

Under the same conditions, heating at reflux of compound **8e** with **5** in absolute ethanol afforded the corresponding malonic acid pyridinium derivative MPQ$^+$ **13** in 42% yield. The IR spectra of the prepared MPQ$^+$ derivative **13** exhibited a strong stretching band at 1690 cm^{-1}, which is attributed to the ν (C=O) stretching of the acid and another absorption band at 1650 cm^{-1}, related to the ν (C=O) of the amide moiety. The ^{1}H NMR spectra for compound **13** showed a singlet signal at δ 6.4 ppm, related to the CH proton of malonic acid moiety attached to the pyridinium nitrogen. The high deshielding character of this CH proton is attributed to the formation of quaternary pyridinium salt and its adjacent to two electronegative COOH groups. Broad signals appear in the offset region at δ 11.8 and 12.4 ppm, which are related to the presence of OH and NH protons, respectively. The protons belonging to the aromatic system and azomethine were observed at the expected chemical shifts and integral values. Mass spectrum and elemental analysis clearly supports the proposed structure. The decarboxylation process did not occur during the preparation of compound **13** and this may be attributed to the basic characters of the dimethyl amino group in compound **8e**.

Reduction of *N*-methyl quaternary pyridinium derivatives **11a–d** and MPQ$^+$ **13** with sodium dithionite in CH_2Cl_2 in the presence of $NaHCO_3$ under atmosphere of N_2 afforded the corresponding *N*-methyl PCDSs **12a–d** and MPCDS **14**, respectively in 40–50% yield (Scheme 3).[27]

Another group of the designed quaternary compounds MEPCDSs (**19a**,**b** Scheme 4) were successfully synthesized. Heating at reflux of nicotinamide **15** with hydrazine monohydrate in absolute ethanol for 5 h affording the corresponding nicotinic acid hydrazide **16** in 85% yield.[28] Heating at reflux of the hydrazide **16** with different aldehydes including 2-hydroxybenzaldehyde **7a**[29] and 4-methoxybenzaldehyde **7b**[30] in absolute ethanol for 5 h to afford the corresponding benzylidenenicotinic acid hydrazide derivatives **17a–b** in 60–77% yield.

Heating at reflux of compounds **17a**,**b** with 2-bromomalonic acid monoethyl ester **3** in absolute ethanol for 30 h afforded the corresponding MEPQ$^+$ **18a**,**b** in 50–75% yield. The IR spectra of the prepared compounds **18a**,**b** showed an absorption band at 1730 cm^{-1}, which is related to ν (C=O) stretching of the acid moi-

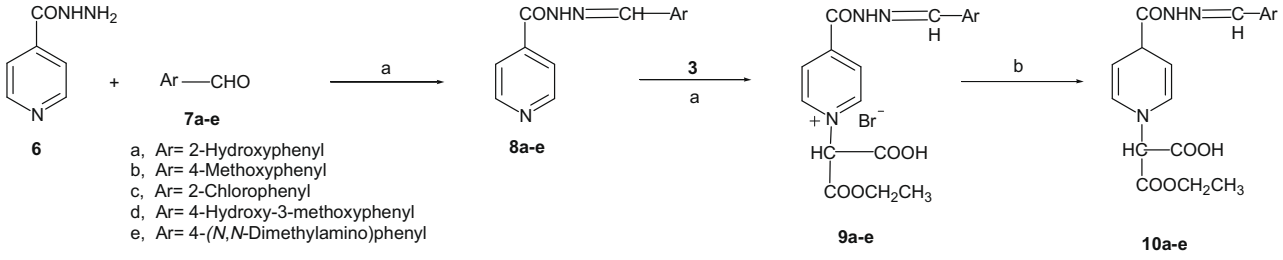

Scheme 2. Synthesis of MEPCDSs **10a–e**. Reagents: (a) EtOH, reflux; (b) $Na_2S_2O_4$, $NaHCO_3$, CH_2Cl_2, N_2 gas.

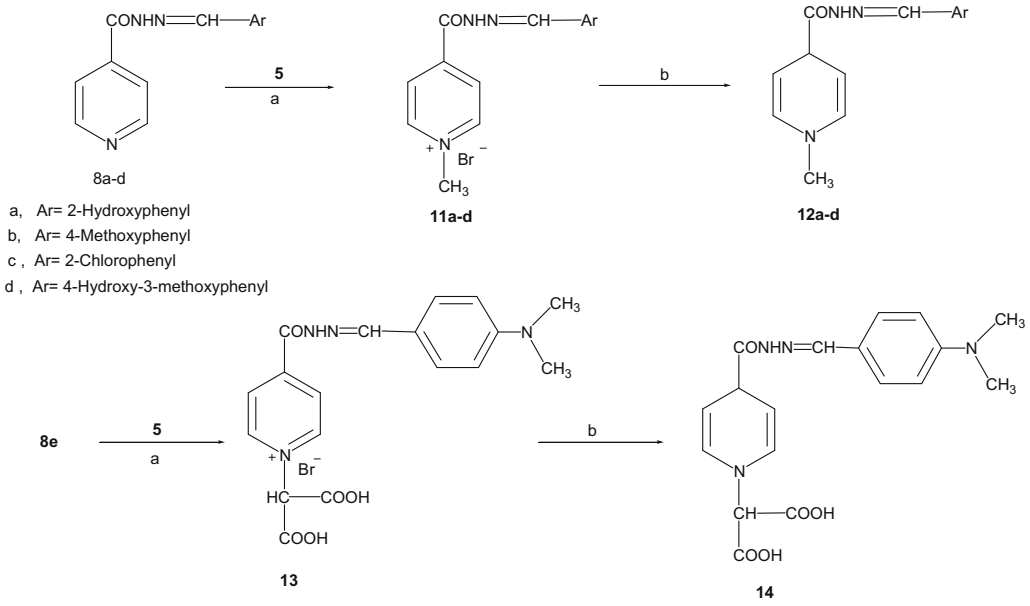

Scheme 3. Synthesis of *N*-methyl PCDSs derivatives **12a–d** and MPCDS **14**. Reagents: (a) EtOH, reflux; (b) $Na_2S_2O_4$, $NaHCO_3$, CH_2Cl_2, N_2 gas.

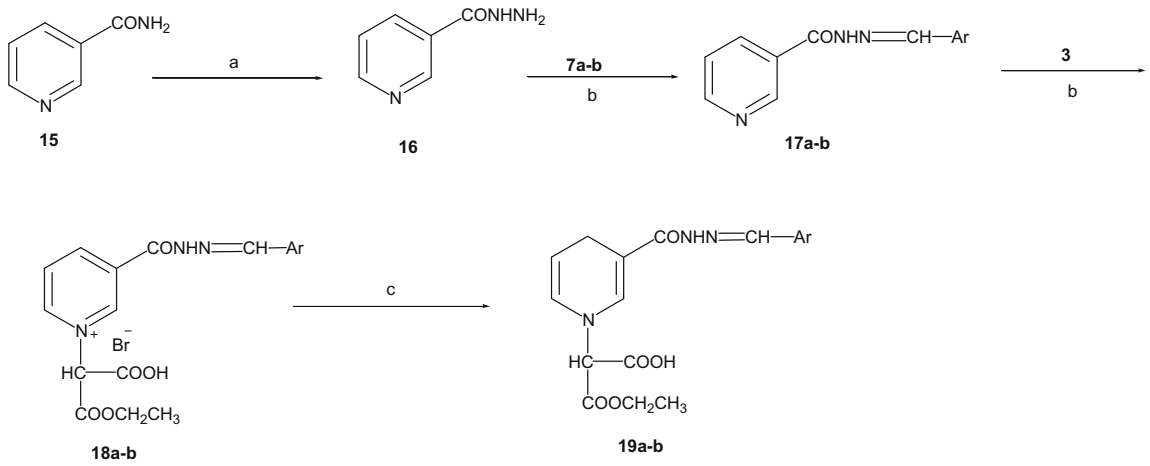

Scheme 4. Synthesis of MEPCDSs **19a**,**b**. Reagents: (a) $NH_2NH_2{\cdot}H_2O$, EtOH, reflux; (b) EtOH, reflux; (c) $Na_2S_2O_4$, $NaHCO_3$, CH_2Cl_2, N_2 gas.

ety, and another stretching band at 1744 cm^{-1} which is related to the ν (C=O C=O) of ester moiety. A strong absorption band at 1671 cm^{-1}, which is attributed to the ν (C=O) of the amide moiety, another broad bands in the region of 3000–3402 cm^{-1} which are related to ν (NH) and ν (OH) stretching. The ^1H NMR spectra recorded for the prepared quaternary compounds **18a**,**b** showed prominent triplet signals of the CH_3 protons at δ 1.1–1.3 ppm and quartet signals at δ 4.2–4.3 ppm indicating the 2 protons of CH_2. A characteristic downfield shifted signal corresponding to the CH protons directly attached to the pyridinum nitrogen was observed at δ 5.7 ppm. The protons belonging to the aromatic system and azomethine were observed at the expected chemical shifts and integral values.

Reduction of the prepared $MEPQ^+$ **18a**,**b** with sodium dithionite in CH_2Cl_2 in the presence of $NaHCO_3$, under atmosphere of nitrogen afforded the corresponding MEPCDSs **19a**,**b** in 60–70% yield[27] (Scheme 4).

2.2. Biological investigations

A group of the prepared 1-malonyl-1,4-dihydropyridine derivatives including; **10a**, **10c**, **12c**, **14**, **19a** and **19b** was subjected to various chemical and biological investigations including; chemical oxidation with ferricyanide and 30% H_2O_2, stability in phosphate buffer (0.2 M, of pHs 7.4 and 5.8), in vitro studies with 80% mice plasma and 20% brain homogenate and in vivo studies to explore these compounds as potential carrier model for brain-specific delivery. Moreover, to evaluate the ability of these compounds to cross the blood–brain barrier, and to be oxidized into their corresponding quaternary derivatives. In this study, high performance liquid chromatography (HPLC) was used to detect and monitor the oxidation of the tested 1-malonyl 1,4-dihydropyridine derivatives into their corresponding quaternary derivatives either chemically or in biological fluids. MeOH/H_2O (50:50) and 0.1% triflouroacetic acid was found to be the most suitable system for running. Experimental parameters including mobile phase, flow rate, type of column and the linearity range were studied in order to determine the optimal conditions for the assay procedure. The HPLC analysis showed that 1-malonyl-1,4-dihydropyridine derivatives were separated from plasma and brain homogenate at retention times (9.16–15.96 min). Their corresponding quaternary derivatives were separated at (3.55–4.98 min). The chromatographic system used allowed a complete base line separation with good resolution of the peaks. The mean calibration curve was plotted; the mean best-fit linear regression equation was derived, and used to estimate the concentrations of the quaternary salts.

2.2.1. Chemical oxidation

2.2.1.1. Oxidation with ferricyanide[31]. The ferricyanide oxidation of dihydropyridine derivatives is commonly used to study their sequential electron–proton–electron transfer mechanism.[32] In the present study, ferricyanide oxidation rates of the prepared MEPCDSs **10a**, **10c**, **12c**, **14**, **19a** and **19b** were investigated spectrophotometrically by monitoring the absorbance of MEPCDSs against time. The test was carried out by mixing freshly prepared MEPCDSs with ferricyanide solution in a concentration of (2×10^{-1} mmol). Either the decrease of absorption of the dihydro derivative (MEPCDSs) or the increase of the absorption of the quaternary ones ($MEPQ^+$) was monitored in the UV region at specific λ_{max} (330, 335, 300, 370, 290 and 295) for MEPCDSs **10a**, **10c**, **12c**, **14**, **19a** and **19b**, respectively, and λ_{max} (370, 380, 345, 395, 345 and 350) for their corresponding $MEPQ^+$ **9a**, **9c**, **11c**, **13**, **18a** and **18b**, respectively. Pseudo first order rate constants and their $t_{1/2}$ were determined by calculation from linear regression of Ln of absorbance against time; the results were illustrated in Table 1.

Data in Table 1 show that the prepared MEPCDSs have high rate of oxidation in ferricyanide solution and that may be attributed to the presence of carboxylic acid function group. 1-Malonyl-1,4-dihydropyridine derivatives have an *N*-substituted-α-amino acid anion moiety, most α-amino acids exist as zwitterions in biological fluids, which are stabilized by the close locations of the opposite charges and the expected ionic interactions. This may result in reduction of the oxidation potential due to decrease of the energy of the transition state and/or the overall activation energy needed for the reaction.

Upon comparison between different forms of the tested MEPCDSs, compound **14** showed the highest rate of oxidation ($t_{1/2}$ = 1.14 min), which may be attributed to the presence of two carboxylic acid function groups in the tested compound. MEPCDSs **10a**, **19a** and **19b** showed good rate of oxidation but less than

Table 1
The rate of oxidation of prepared MEPCDSs **10a**, **10c**, **12c**, **14**, **19a** and **19b** with ferricyanide solution

Compound	*n*	$K_{disapp.}$ (min^{-1})	$t_{1/2}$ (min)	*r*
10a	6	0.28	2.48	0.994
10c	6	0.23	3.01	0.995
12c	6	0.21	3.3	0.984
14	6	0.61	1.14	0.958
19a	6	0.32	2.17	0.999
19b	6	0.33	2.1	0.999

MPCDS **14** ($t_{1/2}$ = 2.48, 2.17 and 2.10 min, respectively) that could be attributed to the presence of only one carboxylic acid function group in these compounds. MEPCDSs **10c** and **12c** showed the lowest rate of oxidation of the tested compounds due to the absence of carboxylic acid function group in these compounds ($t_{1/2}$ = 3.01 and 3.30 min, respectively).

2.2.1.2. Oxidation with hydrogen peroxide (30%). Hydrogen peroxide oxidizes the dihydropyridines by a free radical mechanism, which is the mechanism of air oxidation of these derivatives. Accordingly; this test may be used in accelerated stability studies to compare between different forms of dihydropyridines with respect to their shelf-life stability against air oxidation. In this test, an aliquot of 30% solution of hydrogen peroxide is added to methanolic solution of the MEPCDSs **10a**, **10c**, **12c**, **14**, **19a** and **19b** with a concentration of (2×10^{-1} mmol). The decrease of absorption of the MEPCDSs derivatives or the increase of the absorption of the $MEPQ^+$ was monitored spectrophotometrically in the UV region at specific λ_{max} (330, 335, 300, 370, 290 and 295) for MEPCDS **10a**, **10c**, **12c**, **14**, **19a** and **19b**, respectively and λ_{max} (370, 380, 345, 395, 345 and 350) for their corresponding $MEPQ^+$ **9a**, **9c**, **11c**, **13**, **18a** and **18b**, respectively. Pseudo first order rate constants and their $t_{1/2}$ were determined by calculation from linear regression of Ln of absorbance against time; the results were illustrated in Table 2.

The results of oxidation with hydrogen peroxide showed high rate of oxidation of the prepared MEPCDSs in 30% H_2O_2 but lower than ferricyanide oxidation. MPCDS **14** exhibited the highest rate of oxidation ($t_{1/2}$ = 3.15 min) that could be attributed to the presence of dicarboxylic acid function group. Compounds **10a**, **10c**, **19a** and **19b** exhibited moderate rate of oxidation ($t_{1/2}$ = 3.35, 3.85, 4.08, 5.30 min, respectively) that may be attributed to the presence of only one carboxylic acid function group. Compound **12c** exhibited the lowest rate of oxidation of the tested MEPCDSs ($t_{1/2}$ = 6.30 min) that may be attributed to the absence of carboxylic acid function group.

2.2.2. Stability in buffer solution (shelf-life stability)

Stability of redox-carrier system in buffers of different pHs is usually carried out to investigate the suitable pH for their formulations and to expect their shelf life stability. The stability of MEPCDSs **10c**, **14** and **19b** was investigated in different phosphate buffer (0.2 M, pHs 7.4 and 5.8) at room temperature (32 ± 2 °C). Solutions of different MEPCDSs **10c**, **14** and **19b** with a concentration (2×10^{-1} mmol) in phosphate buffers of different pHs (0.2 M, pHs 7.4 and 5.8) were monitored for 4 days using HPLC for both concentrations of the parent MEPCDSs and for their oxidation or degradation products. Pseudo first order rate constants of disappearance of different MEPCDSs was calculated by linear regression of Ln of its peak areas against time, $t_{1/2}$ was calculated and the results are listed in Table 3.

The results of the stability of different MEPCDS **10c**, **14** and **19b** in phosphate buffers of different pHs revealed that; all of the tested MEPCDSs were stable in both phosphate buffers of pH 7.4 and 5.8, but the stability was higher at phosphate buffer of pH 7.4 compared to pH of 5.8 and that could be attributed to acid catalyzed hydration of the prepared MEPCDS in acidic pH.

2.2.3. In vitro stability in biological fluids

The in vitro stability studies of the redox chemical delivery systems and their corresponding quaternary derivatives in biological fluids, for example, plasma, blood, brain homogenate, are routinely carried out to investigate the transformation pathways of the carrier system in these media and if there will be in vivo site-specific conversion of the dihydro derivative into the corresponding quaternary. In this investigation, the model MEPCDSs were subjected to in vitro stability studies in 80% mice plasma, and 20% mice brain homogenate. Scheme 5 illustrates the expected metabolic pathways of the tested MEPCDSs.

The study of the stability of different MEPCDSs and its corresponding quaternary derivatives $MEPQ^+$s in plasma gives an idea about their comparative stability against enzymatic hydrolysis (K_2 and K_3) by esterase predominant in plasma, since minimal oxidation is expected. On the other hand, investigation of their stabilities in brain homogenate demonstrates the susceptibility of the system components to oxidation by flavin dehydrogenases (K_1 and K_4). From the obtained results, it is possible to determine which comes first, in vivo in the brain, whether hydrolysis of the MEPCDSs or its oxidation to the corresponding $MEPQ^+$.

2.2.3.1. Stability in 80% mice plasma. The stability of both MEPCDSs **10c**, **14** and **19b** and their corresponding $MEPQ^+$ **9c**, **13** and **18b** was investigated in 80% mice plasma at 37 °C, with respect to the tested MEPCDSs, Results revealed that, no quaternary ester ($MEPQ^+$) peak was detected, but only a peak corresponding to the quaternary acid (MPQ^+) was observed, no other peaks were detected in the spectrum. These results suggest that the possible metabolic pathway in plasma is hydrolysis prior to oxidation. Pseudo first order rate constants of disappearances ($K_{disapp.}$) of the tested MEPCDSs, mainly due to hydrolysis (K_2), was found to be $K_{disapp.}$ 2.97×10^{-2} min^{-1} and its $t_{1/2}$ = 23.33 min; while hydrolysis of the quaternary (K_3) was 4.44×10^{-2} min^{-1} and its $t_{1/2}$ = 15.75 min.

Several conclusions could be deduced from these results; first, the rate of hydrolysis of the tested MEPCDSs in plasma is about 17 times faster than rate of its hydrolysis in phosphate buffer of

Table 2
The rate of oxidation of prepared MEPCDSs **10a**, **10c**, **12c**, **14**, **19a** and **19b** with 30% hydrogen peroxide

Compound	n	$K_{disapp.}$ (min^{-1})	$t_{1/2}$ (min)	r
10a	6	0.17	4.08	0.996
10c	6	0.13	5.30	0.997
12c	6	0.11	6.30	0.974
14	6	0.22	3.15	0.993
19a	6	0.18	3.85	0.994
19b	6	0.21	3.35	0.998

Table 3
Stability of different MEPCDSs **10c**, **19** and **25b** in phosphate buffer (0.2 M, pHs 7.4 and 5.8)

Phosphate buffer (0.2 M, pHs)	Compound	n	K_{disapp} ± SD (h^{-1})	$t_{1/2}$ (min)	r
pH 7.4	**10c**	4	0.1034 ± 0.003	402.13	0.997
	14	4	0.1677 ± 0.001	247.94	0.999
	19b	4	0.160 ± 0.004	259.88	0.997
pH 5.8	**10c**	4	0.165 ± 0.001	252	0.999
	14	4	0.2465 ± 0.003	169.29	0.999
	19b	4	0.2117 ± 0.003	196.4	0.999

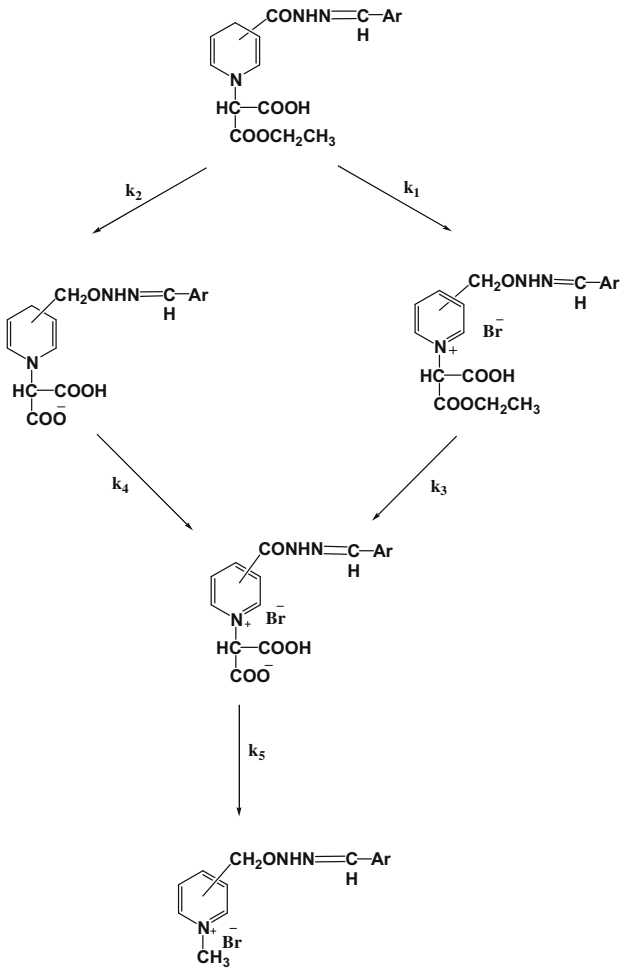

Scheme 5. The expected metabolic pathways of the tested MEPCDSs.

pH 7.4, which illustrates the importance of enzymatic hydrolysis studies on ester type CDSs. Second, close enzymatic rates of hydrolysis of both MEPCDSs and its corresponding $MEPQ^+$, in spite of the activating positive charge on the quaternary molecule. Finally, although the rate of hydrolysis of the MEPCDSs in plasma is fast enough for hydrolysis to precede oxidation, it is relatively reasonable to give enough time for the dihydro-ester to be distributed and reach the brain before complete hydrolysis ($t_{1/2}$ = 18.88–23.33 min). Pseudo first order rate constants of disappearances ($K_{disapp.}$) of the MEPCDSs and their $t_{1/2}$ were calculated by linear regression of Ln of peak area against time in minutes. Table 4 shows the results of the test with MEPCDSs **10c**, **14** and **19b**.

The results showed that MEPCDS **14** exhibited the fastest rate of oxidation in plasma ($t_{1/2}$ = 18.88 min) followed by MEPCDS **19b** ($t_{1/2}$ = 21.81 min) and finally MEPCDS **10c** with a rate of oxidation ($t_{1/2}$ = 23.33 min).

2.2.3.2. Stability in 20% brain homogenate. MEPCDSs **10c**, **14** and **19b** and their corresponding $MEPQ^+$ **9c**, **13** and **18b** were investigated for their stabilities in 20% mice brain homogenates. Mice were sacrificed by decapitation and their brains were isolated and homogenized with isotonic phosphate buffer (0.2 M, pH 7.4). Methanolic solution of MEPCDSs **10c**, **14** and **19b** were added to the homogenate at different time intervals. The supernatants were analyzed by HPLC for their contents of MEPCDSs and their corresponding $MEPQ^+$s. Both of the $K_{disapp.}$ and $t_{1/2}$ of oxidation of the MEPCDSs were calculated by linear regression of Ln of peak areas against time in min. Table 5 shows the results of the test with MEPCDS **10c**, **14** and **19b**.

In mice brain homogenate, the $MEPQ^+$ was hydrolyzed with a pseudo first order rate constant of disappearance K_3 of $K_{disapp.}$ 3.4×10^{-2} min^{-1} and its $t_{1/2}$ = 20.38 min and the rate of appearance of the quaternary acid (MPQ^+) (K_3–K_5) of $K_{disapp.}$ 6.49×10^{-2} min^{-1} and its $t_{1/2}$ = 10.68 min). The above data showed that the tested MEPCDSs exhibited fast rate of oxidation in brain than in plasma and these results emphasize the 'lock-in' mechanism of the tested MEPCDSs. As the drug reaches the brain, it is readily oxidized to give its corresponding $MEPQ^+$, which is hydrophilic enough not to pass the BBB and so become locked in the brain affording its expected effect.

From the above data it is clear that all of the tested MEPCDSs **10c**, **14** and **19b** exhibited high rate of oxidation and their $t_{1/2}$ were found to be around 10 min. With respect to the stability of the tested MEPCDSs, it was interesting to observe that the system is more stable in 20% mice brain homogenate than that in 80% mice plasma ($t_{1/2}$ = 9.58 and 18.88 min, respectively) for compound **14**. Hydrolysis (K_2) may be the main route of its transformation in brain and that is why its rate of hydrolysis in plasma is higher since the concentration of esterase in plasma is higher. No dihydroacid derivative could be detected during the investigation. This proves that once the ester is hydrolyzed, the product is immediately oxidized to the corresponding quaternary acid. Accordingly, the sequential distribution, hydrolysis and oxidation scenario may be accomplished.

2.2.4. In vivo distribution study

Compounds **10c** and **14** were selected for in vivo study, the purpose of this study is to prove that the tested compounds would be able to deliver the corresponding MPQ^+ in a good concentration to the brain and as a result of its hydrophilic character, it will be 'locked-in' there.[33]

Freshly prepared MEPCDSs **10c** or **14** were injected through the external jugular vein as solution in DMF to a group of male Sprague-Dawley rats at a dose level of 20 mg/kg body weight. At specific time intervals, the injected animals were sacrificed and both of their brains and blood samples were collected, and analyzed by HPLC for the appearance of the quaternary acid derivatives MPQ^+. The results of the in vivo experiments of MEPCDS **10c** and **14** are given in Figures 2 and 3.

Neither MEPCDSs nor its hydrolysis product could be detected in blood or brain at any time point, only the quaternary acid could be detected. The concentration of the quaternary acid in blood was found to decrease very quickly to undetectable levels within the first 45 min for both MEPCDSs **10c** and **14**, while its concentration in brain was highest at 20 min and decrease slowly for both MEPCDSs **10c** and **14**. This trend is typical with the 'locking-in'

Table 4
Stability of different MEPCDSs **10c**, **14** and **19b** in 80% mice plasma

Compound	n	K_{disapp} ± SD (min^{-1})	$t_{1/2}$ (min)	r
10c	4	0.0297 ± 0.0013	23.33	0.997
14	4	0.0367 ± 0.0011	18.88	0.998
19b	4	0.03178 ± 0.0004	21.81	0.999

Table 5
Stability of different MEPCDSs **10c**, **14** and **19b** in 20% mice brain homogenate

Compound	n	K_{disapp} ± SD (min^{-1})	$t_{1/2}$ (min)	r
10c	4	0.06489 ± 0.0023	10.679	0.997
14	4	0.07234 ± 0.0106	9.58	0.959
19b	4	0.0683 ± 0.00265	10.146	0.997

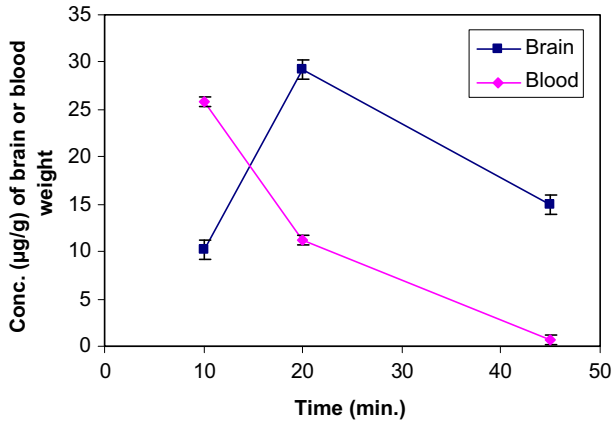

Figure 2. In vivo distribution of MEPCDS **10c** in blood and rat brain homogenate.

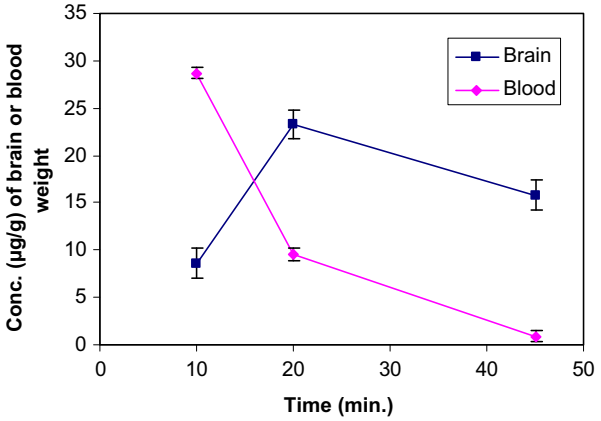

Figure 3. In vivo distribution of MPCDS **14** in blood and rat brain homogenate.

property of the brain-specific chemical delivery systems. Without the involvement of active transport systems or the use of the redox-CDSs, no drug can reach significantly higher concentrations in brain than blood.

To test the efficiency of the tested MEPCDSs **10c** and **14**, the obtained results were compared with reported results of selected efficient PCDSs including dopamine, testosterone, phenethylamine and tryptamine-PCDSs, in which the concentration of the quaternary end products in brain were determined. The overall efficiency of the carrier system can be measured by calculating the ratio of highest concentration of the quaternary in brain to the dose administered, considering the body weight as the theoretical volume of distribution. Table 6 illustrates the results of these calculations.

2.2.5. Antidepressant screening

MEPCDS **10a**, **10c**, **14** and **19a** and their corresponding quaternary MEPQ$^+$ **9a**, **9c**, **13** and **18a** were evaluated for their antidepressant activity using tail suspension behavioral despair test.[37–43]

This test is used effectively in predicting the activity of a wide variety of antidepressants such as MAO inhibitors and tricyclic antidepressants.[37,38] The synthesized compounds **10a**, **10c**, **14**, **19a**, **9a**, **9c**, **13** and **18a** (10 mg/kg), and the tricyclic antidepressant imipramine as a reference drug (10 mg/kg) were dissolved in carboxymethylcellulose (CMC) solution (0.5% w/v in water) and were injected ip in a standard volume of 0.5 mL per 100 g body weight, 1 h prior to the test. Control animals were similarly

Table 6
Comparison of the result of the in vivo distribution studies for different nicotinic acid, 3,5-pyridine dicarboxylic acid carriers, and 1-malonyl-1,4-dihydropyridine CDS

Compound	Dose (mg/kg)	Theoretical max. conc. (µg/g)	Exp. max. conc. (µg/g)	Ratio
DA-CDS[a34]	50	50	22	0.44
T-CDS[b35]	30	30	15	0.50
Ph-CDS[c36]	20	20	9.6	0.48
Try-CDS[d36]	20	20	6.0	0.30
MEPCDS 10c	20	20	23.23	1.16
MEPCDS 14	20	20	29.17	1.46

[a] Dopamine CDS.
[b] Testosterone CDS.
[c] Phenethylamine CDS.
[d] Tryptamine CDS.

treated with CMC solution (0.5% w/v in water). One hour later, the mice were suspended by the tail to the edge of a shelf 80 cm above the floor. The tail was secured to the shelf by adhesive tape placed approximately 1 cm from the tip of the tail. The duration of the immobility was recorded over a period of 6 min. Mice were considered immobile only when they hung passively and completely motionless.

Results of the antidepressant activity of the tested compounds and reference drug are given in Table 7. MEPCDSs **19a** and **14** and the MEPQ$^+$ **13** induced remarkable antidepressant activity compared to imipramine. Compounds **13**, **14** and **19a** significantly reduced the duration of immobility times to be 85.30, 108.40 and 118.50 s, respectively, compared to 132.00 s reduction of the duration of immobility for imipramine. MEPCDSs **10a**, **10c** and MEPQ$^+$ **18a** induce good antidepressant activity, their activities nearly equal to 92.8%, 86.7% and 90.20% of the activity of imipramine. Other MEPQ$^+$ including **9a** and **9c** exhibited moderate antidepressant activity, their activities nearly equal to 78.80% and 79.60% of the activity of imipramine. Moreover, the results of the antidepressant activities of the tested MEPCDSs revealed that the MEPCDS **19a** exhibited the highest antidepressant activity compared to other tested MEPCDSs (Figure 4A). The MEPQ$^+$ **13** exhibited the highest antidepressant activity compared to other tested MEPQ$^+$ (Figure 4B). The results of the antidepressant activities also revealed that MEPCDS **10a**, **10c**, **14** and **19a** exhibited good antidepressant activities better than their corresponding MEPQ$^+$ **9a**, **9c**, **13** and **18a** (Figure 4C) and that reflects the importance of the chemical delivery system for delivering drugs to the brain. The results of comparison between different MEPCDS **10a**, **10c**, **14** and **19a** and their corresponding MEPQ$^+$ **9a**, **9c**, **13** and **18a** are listed in Table 7 and shown in Figures 4A–C

Table 7
Effect of the tested compounds **10a**, **10c**, **14**, **19a**, **9a**, **9c**, **13** and **18a** and imipramine on the duration of immobility in mice using tail suspension technique

Compound	Duration of immobility (s) (mean ± S.E.M.)	% Deviation from control
Control	240.6 ± 14.93	0.00
Imipramine	132 ± 0.0	−45.14
9a	167.6 ± 3.225	−30.34
9c	165.8 ± 5.87	−31.42
13	118.5 ± 10.13	−50.75
18a	146.4 ± 3.44	−39.15
10a	152.3 ± 4.66	−36.7
10c	142.2 ± 15.9	−40.9
14	108.4 ± 4.24	−54.95
19a	85.3 ± 17.24	−64.55

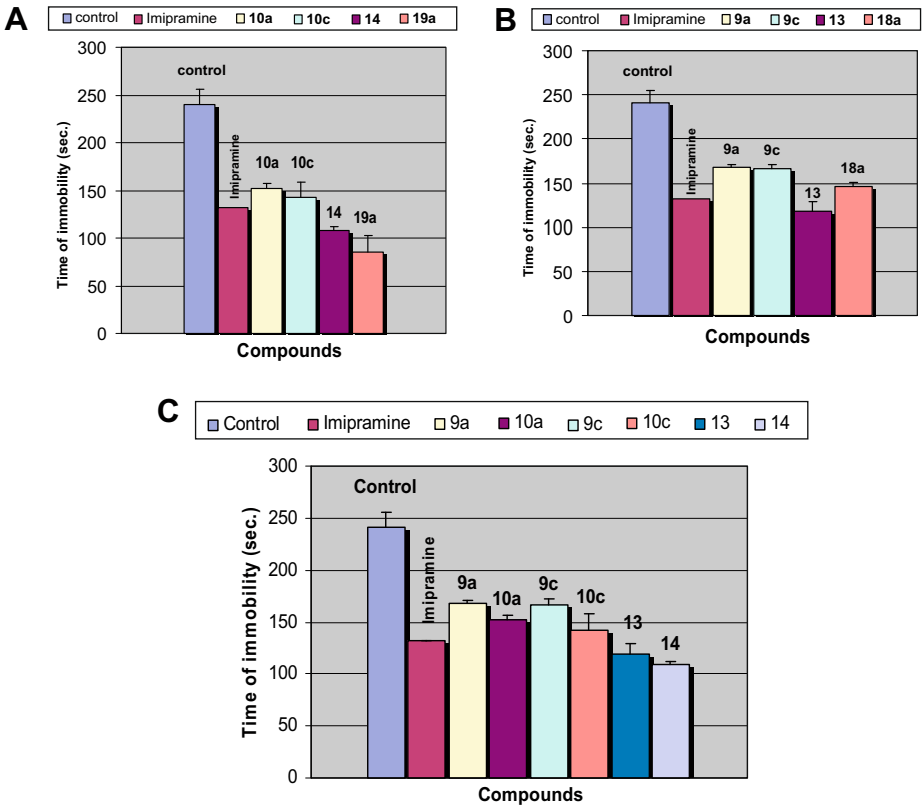

Figure 4. The antidepressant activities of different MEPCDSs **10a**, **10c**, **14**, **19a** and MEPQ$^+$s **9a**, **9c**, **13**, **18a** compared to imipramine at a dose level of 10 mg/kg. (A) The antidepressant activities of different MEPCDSs **10a**, **10c**, **14**, **19a** compared to imipramine at a dose level of 10 mg/kg. (B) The antidepressant activities of different MEPQ$^+$s **9a**, **9c**, **13**, **18a** compared to imipramine at a dose level of 10 mg/kg. (C) The antidepressant activities of MEPCDSs **10a**, **10c**, **14** and their corresponding MEPQ$^+$s **9a**, **9c**, **13** compared to imipramine at a dose level of 10 mg/kg.

3. Experimental

3.1. Chemistry

Reactions were monitored by TLC analysis using Merck 9385 pre-coated aluminum plate Silica Gel (Kieselgel 60) with F_{254} indicator thin layer plates. Melting points were determined on Stuart electrothermal melting point apparatus and were uncorrected. IR spectra were recorded as KBr disks on a Brukar Vector 22 IR spectrophotometer. ^{1}H NMR spectra were carried out on 200 MHz GEMINI-200 NMR spectrophotometer and on 60 MHz Varian EM-360L NMR spectrophotometer using TMS as internal reference. Chemical shifts (δ values are given in parts per million (ppm) using $CDCl_3$ (7.29) or DMSO-d_6 (2.5) as solvents and coupling constants (J) in Hertz. Splitting patterns are designated as follows: s, singlet; d, doublet; t, triplet; q, quartet; dd, doublet of doublet; m, multiplet.

Accurate masses were obtained on HP mass spectrometer. Elemental analysis was performed on Perkin Elmer 2400 CHN Elemental analyzer and on Vario EL III, Elemental analyzer, GMBH. D-63452 HANAU.

3.1.1. Synthesis of 2-bromomalonic acid monoethyl ester 3 and 2-bromomalonic acid 5[20,21]

3.1.2. Synthesis of nicotinic acid hydrazide 16.[28]

To a stirred solution of nicotinamide **15** (1.22 g, 10.0 mmol) in 20 mL absolute ethanol, hydrazine monohydrate 98% (0.98 g, 20.0 mmol) was added. The mixture was heated at reflux for about 6 h, the solvent was evaporated under reduced pressure and the resulting solid was filtered off and crystallized from ethanol affording **16** as white crystals in (1.16 g, 85% yield), mp 102 °C.

3.1.3. General procedure for synthesis of benzylideneisonicotinic acid hydrazides 8a–e

To a stirred solution of isonicotinic acid hydrazide **6** (1.37 g, 10.0 mmol) in 30 mL absolute ethanol, the aromatic aldehyde **7a–e** was added (10.0 mmol). The mixture was heated at reflux for 5–7 h. The obtained precipitate was filtered off and crystallized from ethanol.

3.1.3.1. (2-Hydroxybenzylidene)isonicotinic acid hydrazide 8a[22]. Yellowish white crystals in (1.93 g, 80% yield); mp 253–255 °C. ^{1}H NMR (60 MHz, DMSO-d_6) δ (ppm): 7.3–9.7 (m, 9H, Ar-H, –N=*CH*-Ar), 12.3 (br s, 1H, OH), 13.1 (br s, 1H, NH).

3.1.3.2. (4-Methoxybenzylidene)isonicotinic acid hydrazide 8b[23]. Yellowish white crystals in (1.78 g, 70% yield); mp 171–172 °C. ^{1}H NMR (60 MHz, DMSO-d_6) δ (ppm): 3.8 (s, 3H, OCH_3), 7.3–9.8 (m, 9H, Ar-H, –N=*CH*-Ar), 12.1 (br s, 1H, NH).

3.1.3.3. (2-Chlorobenzylidene)isonicotinic acid hydrazide 8c[24]. White crystals in (2.13 g, 82.2% yield); mp 216–217 °C. ^{1}H NMR (60 MHz, DMSO-d_6) δ (ppm): 7.7–9.9 (m, 9H, Ar-H, –N=*CH*-Ar), 13.1 (br s, 1H, NH).

3.1.3.4. (4-Hydroxy-3-methoxybenzylidene)isonicotinic acid hydrazide 8d[25]. Yellow crystals in (1.84 g, 68% yield); mp 238–240 °C. ^{1}H NMR (60 MHz, DMSO-d_6) δ (ppm): 4.3 (s, 3H, OCH_3), 7.3–9.8 (m, 9H, Ar-H, –N=*CH*-Ar), 12.5 (br s, 1H, NH).

3.1.3.5. (4-Dimethylaminobenzylidene)isonicotinic acid hydrazide 8e[26]. Yellow crystals in (1.61 g, 60% yield); mp 189–190 °C.

^{1}H NMR (60 MHz, DMSO-d_6) δ (ppm): 3.4 [s, 6H, N–$(CH_3)_2$], 7.1–9.6 (m, 9H, Ar-H, –N=*CH*-Ar), 12.6 (br s, 1H, NH).

3.1.4. General procedure for synthesis of benzylidenenicotinic acid hydrazides 17a,b

An equimolar mixture of nicotinic acid hydrazide **16** (1.37 g, 10.0 mmol) and different aromatic aldehydes **7a**,**b** (10.0 mmol) in 30 mL absolute ethanol was heated at reflux for 10 h. The resulting solid was filtered off and crystallized from ethanol.

3.1.4.1. (2-Hydroxybenzylidene)nicotinic acid hydrazide 17a[29]. Yellowish white crystals in (1.86 g, 77.2% yield); mp 185–186 °C. ^{1}H NMR (60 MHz, DMSO-d_6) δ (ppm): 7.3–10.2 (m, 9H, Ar-H, –N=*CH*-Ar), 12.5 (br s, 1H, OH), 13.0 (br s, 1H, NH).

3.1.4.2. (4-Methoxybenzylidene)nicotinic acid hydrazide 17b[30]. Yellow crystals in (1.53 g, 60% yield); mp 177–180 °C. ^{1}H NMR (60 MHz, DMSO-d_6) δ (ppm): 4.2 (s, 3H, OCH_3), 7.3–9.8 (m, 9H, Ar-H, –N=*CH*-Ar), 12.1 (br s, 1H, NH).

3.1.5. General procedure for synthesis of 1-(carboxyethoxycarbonylmethyl)-4-(benzylidenehydrazino-carbonyl)pyridinium bromide derivatives 9a–e

To a stirred solution of the prepared benzylideneisonicotinic acid hydrazides **8a**–**e** (10.0 mmol) in 30 mL absolute ethanol, a solution of 2-bromomalonic acid monoethyl ester **3** (20.0 mmol) in 30 mL absolute ethanol was added and the mixture was heated at reflux for 48 h. The solution was concentrated under reduced pressure and the resulting solid was filtered off and crystallized from ethanol/diethyl ether.

3.1.5.1. 1-(Carboxyethoxycarbonylmethyl)-4-[(2-hydroxybenzylidene)hydrazinocarbonyl]pyridinium bromide 9a. Orange crystals in (1.81 g, 40% yield); mp 210–211 °C. IR (KBr) ν_{max} (cm^{-1}): 1680 (C=O amide), 1735 (C=O acid), 1755 (C=O ester), 3050 (OH), 3450 (NH). ^{1}H NMR (200 MHz, DMSO-d_6) δ (ppm): 1.29 (t, 3H, J = 7.4 Hz, CH_3), 4.3 (q, 2H, J = 7.4 Hz, CH_2), 5.76 (s, 1H, CH), 6.9–9.4 (m, 9H, Ar-H, –N=*CH*-Ar), 10.8 (br s, 1H, COOH), 12.8 (br s, 1H, NH). ^{13}C NMR (100 MHz, DMSO-d_6) δ 13.63 (CH_3), 63.72 (CH_2), 72.1 (CH), 116.35 (CH), 118.59 (C–CH=N), 119.33 (CH), 121.45 (CH), 129.12 (CH), 131.63 (CH), 139.99 (C–CO), 148.91 (CH), 149.29 (C), 150.19 (CH), 157.88 (CO), 160.38 (CO), 162.09 (CO). MS: *m*/*z* (%) 241 (25.9) [M^+−211], 123 (79.2), 106 (100), 78.3 (67.9). Anal. Calcd for $C_{18}H_{18}BrN_3O_6$: C, 47.80; H, 4.01; N, 9.29. Found: C, 48.06; H, 3.95; N, 9.56.

3.1.5.2. 1-(Carboxyethoxycarbonylmethyl)-4-[(4-methoxybenzylidene)hydrazinocarbonyl]pyridinium bromide 9b. Yellow crystals in (3.27 g, 70.1% yield); mp 186–188°C. IR (KBr) ν_{max} (cm^{-1}): 1678 (C=O amide), 1745 (C=O acid), 1755 (C=O ester), 3127 (OH), 3451 (NH). ^{1}H NMR (200 MHz, DMSO-d_6) δ (ppm): 1.28 (t, 3H, J = 7.0 Hz, CH_3), 3.83 (s, 3H, OCH_3) 4.27 (q, 2H, J = 7.0 Hz, CH_2), 5.74 (s, 1H, CH), 6.9–9.4 (m, 9H, Ar-H, –N=*CH*-Ar), 12.2 (br s, 1H, COOH), 12.44 (br s, 1H, NH). ^{13}C NMR (100 MHz, DMSO-d_6) δ 14.1 (CH_3), 55.77 (OCH_3), 64.19 (CH_2), 72.51 (CH), 114.85 (CH), 125.81 (CH), 126.47 (C), 129.61 (CH), 148.42 (CH), 150.12 (C), 150.88 (CH), 152.52 (C), 158.85 (CO), 161.83 (CO), 162.57 (CO). MS: *m*/*z* (%) 255.2 (11.7) [M^+−211], 133.2 (100), 106 (37.3), 78.3 (48.4). Anal. Calcd for $C_{19}H_{20}BrN_3O_6$: C, 48.94; H, 4.32; N, 9.01. Found: C, 48.48; H, 3.91; N, 9.14.

3.1.5.3. 1-(Carboxyethoxycarbonylmethyl)-4-[(2-chlorobenzylidene)hydrazinocarbonyl]pyridinium bromide 9c. Yellowish white crystals in (2.64 g, 56% yield); mp 183–184 °C. IR (KBr) ν_{max} (cm^{-1}): 1682 (C=O amide), 1746 (C=O acid), 1752 (C=O ester), 3122 (OH), 3445 (NH). ^{1}H NMR (200 MHz, DMSO-d_6) δ (ppm): 1.26 (t, 3H, J = 7.2 Hz, CH_3), 4.27 (q, 2H, J = 7.2 Hz, CH_2), 5.75(s, 1H, CH), 7.4–9.3 (m, 9H, Ar-H, –N=*CH*-Ar), 12.3 (br s, 1H, –COOH), 12.8 (br s, 1H, NH). MS: *m*/*z* (%) 259 (36.8) [M^+−211], 122 (40.0), 106 (100.0), 78.3 (58.6). Anal. Calcd for $C_{18}H_{17}BrClN_3O_5$: C, 45.93; H, 3.64; N, 8.93. Found: C, 45.75; H, 3.53; N, 9.05.

3.1.5.4. 1-(Carboxyethoxycarbonylmethyl)-4-[(4-hydroxy-3-methoxybenzylidene)hydrazinocarbonyl]pyridinium bromide 9d. Yellow crystals in (2.41 g, 50% yield); mp 178–180 °C. IR (KBr) ν_{max} (cm^{-1}): 1668 (C=O amide), 1730 (C=O acid), 1739 (C=O ester), 3207 (OH), 3411 (NH). ^{1}H NMR (200 MHz, DMSO-d_6) δ (ppm): 1.28 (t, 3H, J = 7.0 Hz, CH_3), 3.84 (s, 3H, OCH_3), 4.26 (q, 2H, J = 7.0 Hz, CH_2), 5.75 (s, 1H, CH), 6.7–9.3 (m, 8H, Ar-H, –N=*CH*-Ar), 9.8 (s, 1H, OH), 11.9 (br s, 1H, COOH), 12.4 (br s, 1H, NH). MS: *m*/*z* (%) 270 (26.4) [M^+−211], 149 (100), 123 (26.2), 106 (56.5), 78 (74.6). Anal. Calcd for $C_{19}H_{20}BrN_3O_7$: C, 47.32; H, 4.18; N, 8.71. Found: C, 47.29; H, 4.10; N, 8.24.

3.1.5.5. 1-(Carboxyethoxycarbonylmethyl)-4-[(4-dimethylaminobenzylidene)hydrazinocarbonyl]pyridinium bromide 9e. Reddish brown crystals in (2.40 g, 50% yield); mp 216–217 °C. IR (KBr) ν_{max} (cm^{-1}): 1671 (C=O amide), 1740 (C=O acid), 1748 (C=O ester), 3165 (OH), 3429 (NH). ^{1}H NMR (200 MHz, DMSO-d_6) δ (ppm): δ 1.32 (t, 3H, J = 7.2 Hz, CH_3), 3.24 (s, 3H, CH_3), 3.35 (s, 3H, CH_3), 4.4 (q, 2H, J = 7.2 Hz, CH_2), 5.76 (s, 1H, CH), 6.8–9.49 (m, 9H, Ar-H, –N=*CH*-Ar), 12.29 (br s, 1H, CO–OH), 12.52 (br s, 1H, NH). MS: *m*/*z* (%) 268 (61.1) [M^+−211], 146 (100), 106 (13.6), 78 (35.1). Anal. Calcd for $C_{20}H_{23}BrN_4O_5$: C, 50.12; H, 4.84; N, 11.69. Found: C, 50.01; H, 4.78; N, 11.66.

3.1.6. General procedure for synthesis of 1-(carboxyethoxycarbonylmethyl)-3-(benzylidenehydrazino carbonyl)pyridinium bromide derivatives 18a,b

To a stirred solution of the prepared benzylidenenicotinic acid hydrazides **17a**,**b** (10.0 mmol) in 30 mL absolute ethanol, a solution of 2-bromomalonic acid monoethyl ester **3** (20.0 mmol) in 30 mL absolute ethanol was added and the mixture was heated at reflux for 48 h. The solution was concentrated under reduced pressure and the resulting solid was filtered off and crystallized from ethanol/diethyl ether.

3.1.6.1. 1-(Carboxyethoxycarbonylmethyl)-3-[(2-hydroxybenzylidene)hydrazinocarbonyl]pyridinium bromide 18a. Yellowish white crystals in (3.39 g, 75% yield); mp 218–219 °C. IR (KBr) ν_{max} (cm^{-1}): 1671 (C=O amide), 1738 (C=O acid), 1744 (C=O ester), 3137 (OH), 3467 (NH). ^{1}H NMR (200 MHz, DMSO-d_6) δ (ppm): 1.28 (t, 3H, J = 7.1 Hz, CH_3), 4.27 (q, 2H, J = 7.1 Hz, CH_2), 5.77 (s, 1H, CH), 6.95–9.64 (m, 9H, Ar-H, –N=*CH*-Ar), 10.8 (br s, 1H, COOH), 12.3 (br s, 1H, OH), 12.66 (br s, 1H, NH). MS: *m*/*z* (%) 241 (25.9) [M^+−211], 123 (79.2), 106 (100), 78.3 (67.9). Anal. Calcd for $C_{18}H_{18}BrN_3O_6$: C, 47.80; H, 4.01; N, 9.29. Found: C, 48.00; H, 3.88; N, 9.38.

3.1.6.2. 1-(Carboxyethoxycarbonylmethyl)-3-[(4-methoxybenzylidene)hydrazinocarbonyl]pyridinium bromide 18b. Orange red crystals in (2.33 g, 50% yield); mp 147–148 °C. IR (KBr) ν_{max} (cm^{-1}): 1673 (C=O amide), 1730 (C=O acid), 1738 (C=O ester), 3213 (OH), 3402 (NH). ^{1}H NMR (200 MHz, DMSO-d_6) δ (ppm): δ 1.26 (t, 3H, J = 7.1 Hz, CH_3), 3.85 (s, 3H, OCH_3), 4.25 (q, 2H, J = 7.0 Hz, CH_2), 5.78 (s, 1H, CH), 6.9–9.7 (m, 9H, Ar-H, –N=*CH*-Ar), 12.1 (br s, 1H, COOH), 12.48 (br s, 1H, NH). MS: *m*/*z* (%) 255 (10.2) [M^+−211], 133 (100), 106 (63.9), 78 (50.8). Anal. Calcd for $C_{19}H_{20}BrN_3O_6$: C, 48.94; H, 4.32; N, 9.01. Found: C, 48.62; H, 3.91; N, 9.24.

3.1.7. General procedure for synthesis of 1-methyl-4-(benzylidenehydrazinocarbonyl)pyridinium bromide derivatives 11a–d

To a stirred solution of the prepared benzylideneisonicotinic acid hydrazides **8a**–**e** (10.0 mmol) in 30 mL absolute ethanol, a solution of 2-bromomalonic acid **5** (20.0 mmol) in 20 mL absolute ethanol was added. The mixture was heated at reflux for 30 h. The solution was concentrated under reduced pressure and the resulting solid was filtered off and crystallized from ethanol/diethyl ether.

3.1.7.1. 1-Methyl-4-[(2-hydroxybenzylidene)hydrazinocarbonyl]pyridinium bromide 11a. White crystals in (1.34 g, 40% yield); mp 244–245 °C. IR (KBr) ν_{max} (cm^{-1}): 1682 (C=O amide), 3181 (OH), 3441 (NH). ^1H NMR (200 MHz, DMSO-d_6) δ (ppm): δ 4.39 (s, 3H, CH_3), 7.48–9.27 (m, 9H, Ar-H, –N=*CH*-Ar), 11.4 (br s, 1H, OH), 12.2 (br s, 1H, NH). MS: *m*/*z* (%) 241 (16.4) [M^+−211], 123 (87.1), 106 (83.4), 78 (100). Anal. Calcd for $C_{14}H_{14}BrN_3O_2$: C, 50.02; H, 4.20; N, 12.50. Found: C, 50.08; H, 4.30; N, 11.95.

3.1.7.2. 1-Methyl-4-[(4-methoxybenzylidene)hydrazinocarbonyl]pyridinium bromide 11b. Yellowish white crystals in (1.93 g, 55.1% yield); mp 150–152 °C. IR (KBr) ν_{max} (cm^{-1}): 1649 (C=O amide), 3441 (NH). ^1H NMR (200 MHz, DMSO-d_6) δ (ppm): 3.84 (s, 3H, OCH_3), 4.44 (s, 3H, CH_3), 6.49–8.81 (m, 9H, Ar-H, –N=–N=*CH*-Ar), 11.96 (br s, 1H, NH). MS: *m*/*z* (%) 349 (8.1) [M^+], 255 (7.0) [M^+−94], 133 (43.0), 106 (23.3), 93 (100), 78 (34.9). Anal. Calcd for $C_{15}H_{16}BrN_3O_2$: C, 51.44; H, 4.60; N, 12.00. Found: C, 51.51; H, 4.83; N, 12.86.

3.1.7.3. 1-Methyl-4-[(2-chlorobenzylidene)hydrazinocarbonyl]pyridinium bromide 11c. Yellowish white crystals in (1.88 g, 53% yield); mp 250–252 °C. IR (KBr) ν_{max} (cm^{-1}): 1658 (C=O amide), 3423 (NH). ^1H NMR (200 MHz, DMSO-d_6) δ (ppm): 4.44 (s, 3H, CH_3), 7.48–9.27 (m, 9H, Ar-H, –N=*CH*-Ar), 12.76 (br s, 1H, NH). MS: *m*/*z* (%) 356 (9.3) [M^+], 224 (14.7), 122 (52), 106 (100), 78 (70.0). Anal. Calcd for $C_{14}H_{13}BrClN_3O$: C, 47.42; H, 3.69; N, 11.85. Found: C, 47.49; H, 3.56; N, 12.14.

3.1.7.4. 1-Methyl-4-[(4-hydroxy-3-methoxybenzylidene)hydrazinocarbonyl]pyridinium bromide 11d. Yellow crystals in (2.23 g, 61% yield); mp 228–229 °C. IR (KBr) ν_{max} (cm^{-1}): 1664 (C=O amide), 3021 (OH), 3423 (NH). ^1H NMR (200 MHz, DMSO-d_6) δ (ppm): 3.84 (s, 3H, OCH_3), 4.43 (s, 3H, CH_3), 6.89–9.6 (m, 9H, Ar-H, –N=*CH*-Ar), 11.9 (br s, 1H, OH), 12.33 (br s, 1H, NH). MS: *m*/*z* (%) 271 (35.8) [M^+−94], 149 (83.0), 123 (26.4), 106 (77.4), 78 (86.6). Anal. Calcd for $C_{15}H_{16}BrN_3O_3$: C, 49.20; H, 4.40; N, 11.47. Found: C, 48.98; H, 4.28; N, 11.58.

3.1.8. Synthesis of 1-dicarboxymethyl-4-(4,4-dimethylaminobenzylidenehydrazinocarbonyl)pyridinium bromide 13

Compound **13** was prepared according to the general procedure described above for synthesis of compounds **11a**–**d** with a refluxing time of 15 h resulting in a brownish red crystals in (2.4 g, 42% yield), mp 180–182 °C; ν_{max}/cm^{-1} 1642 (C=O amide), 1689 (C=O acid), 3422 (OH), 3495 (NH); ^1H NMR (200 MHz, DMSO-d_6): δ 3.2 (s, 6H, $2CH_3$), 5.64 (s, 1H, CH), 6.52–8.82 (m, 9H, Ar-H, –N=CH-Ar), 11.83 (br s, 1H, NH); MS: *m*/*z* (%) 449 (7.4) [M^{2+}], 289 (3.7), 105 (18.5), 79 (7.4), 56 (100). Anal. Calcd for $C_{18}H_{19}BrN_4O_5$: C, 47.91; H, 4.24; N, 12.42. Found: C, 47.49; H, 4.56; N, 12.35.

3.1.9. General procedure for synthesis 2-[4-(benzylidenehydrazinocarbonyl)-2-(carboxyethoxycarbonylmethyl)-1,4-dihydropyridine 10a–e, 4-(benzylidenehydrazino carbonyl)-1,4-dihydro-*N*-methylpyridine derivatives 12a–d, *N*-(dicarboxymethyl)-1,4-dihydro-4-[(4,4-dimethylamino)benzylidenehydrazinocarbonyl] pyridine 14 and 2-[3-(benzylidenehydrazinocarbonyl)-2-(carboxyethoxycarbonylmethyl)-1,4-dihydropyridine 19a,b[27]

To an ice cooled stirred mixture of compounds **9a**–**e**, **11a**–**d**, **13** or **18a**,**b** (3.00 mmol) in 100 mL deareated water, 200 mL CH_2Cl_2 and sodium bicarbonate (1.1 g; 12.00 mmol) were added. Sodium dithionite (2.1 g; 12.00 mmol) was added gradually to the mixture while stirring, the mixture was stirred under atmosphere of nitrogen gas for 3 h. The red organic layer was separated, washed with 2 × 30 mL water, dried over anhydrous sodium sulfate, filtered and evaporated under reduced pressure to give **10a**–**e**, **12a**–**d**, **14** and **19a**,**b** as yellow orange viscous oily products in 60–70% yield. The obtained products were directly protected from light and kept at (−10 °C) and used directly for further biological investigations.

3.2. Biology

3.2.1. Chemical oxidation

3.2.1.1. Oxidation with ferricyanide. To a series of tubes, each containing 3 mL of freshly prepared ferricyanide reagent, 1 mL of (2×10^{-1} mmol) freshly prepared methanolic solution of MEPCDSs **10a**, **10c**, **12c**, **14**, **19a** and **19b** was added, the mixture was shaken and set aside at room temperature. At a suitable time intervals (5, 10, 20, 45, and 60 min) the tubes were vortexed, filtered and monitored spectrophotometrically for the disappearance of the MEPCDSs and the appearance of their corresponding $MEPQ^+$s at their specific λ_{max}. The rate of disappearance of MEPCDSs and the appearance of their corresponding $MEPQ^+$s were determined. The apparent pseudo first order rate constant of disappearance of MEPCDS ($K_{disapp.}$, min^{-1}) was determined by calculation from linear regression of absorbance against time in min.

3.2.1.2. Oxidation with hydrogen peroxide (30%). In a series of tubes, 1 mL of (2×10^{-1} mmol) freshly prepared methanolic solution of MEPCDSs **10a**, **10c**, **12c**, **14**, **19a** and **19b** was added to 10 mL of 30% H_2O_2 solution. The mixtures were mixed and set aside at room temperature. At the specific time intervals (5, 10, 20, 45, and 60 min) the tubes were vortexed, filtered and monitored spectrophotometrically for the disappearance of the MEPCDSs and the appearance of their corresponding $MEPQ^+$s at their specific λ_{max}. The apparent pseudo first order rate constants of disappearance of MEPCDS ($K_{disapp.}$, min^{-1}) was determined by calculation from linear regression of absorbance against time in minutes.

3.2.1.3. Stability of the prepared MEPCDSs in buffer systems. Two series each of four tubes, each tube contains 5 mL of phosphate buffer of (pH 5.8 or 7.4), 0.5 mL of (2×10^{-1} mmol) freshly prepared methanolic solution of MEPCDSs **10c**, **14** and **19b** was added. The mixtures were kept in dark at room temperature all the time of experiment (4 days). At appropriate time intervals (2, 24, 48, 72, and 96 h), 20 μL of the mixture was taken and analyzed by HPLC for their contents of the MEPCDSs and their corresponding metabolites. The apparent pseudo first order rate constant of disappearance of MEPCDSs ($K_{disapp.}$, min^{-1}) was determined by calculation from linear regression of the Ln of the MEPCDS peak area against time in hours.

3.2.2. In vitro stability in biological fluids

3.2.2.1. Stability in 80% mice plasma. A freshly collected heparinized mice blood was centrifuged at 4000 rpm for 20 min, and the supernatant (plasma) was collected by a Pasteur pipette. To 3 mL of 80% freshly collected plasma diluted with (phosphate buffer 0.11 mol, pH 7.4) pre-warmed in a water bath at 37 °C for 5 min, 300 μL of (2×10^{-1} mmol) methanolic solution of freshly prepared MEPCDSs **10c**, **14** and **19b** was added and mixed thoroughly. The mixture was kept at 37 °C all the time of the experiment. Samples of 200 μL were withdrawn from the tested mixture at different time intervals (1, 2, 4, 8, 16, 32, and 64 min) and added immediately to 2 mL of ice-cooled methanol, vortexes, and places in a deep freezer (−80 °C). When all the samples have

been collected, they were centrifuged, and the supernatants were filtered through nitrocellulose membrane filter (0.22 μm) and analyzed by HPLC for their contents of the MEPCDSs **10c**, **14** and **19b** and their corresponding $MEPQ^+$s derivatives. The apparent pseudo first order rate constant of disappearance ($K_{disapp.}$, min^{-1}) of the MEPCPS was determined by linear regression of the Ln of the MEPCPS peak area against time in minutes.

3.2.2.2. Stability in 20% mice brain homogenate. Ten adult male albino Swiss-Webster mice were sacrificed by decapitation and their brains were removed, washed with ice cold saline solution, weighed (total weight ≈ 4 g) and homogenized in a tissue homogenizer with 20 mL of aqueous ice-cold isotonic phosphate buffer (0.2 mol, pH 7.4), while keeping the homogenizer tube in ice bath during homogenization. To 5 mL of the freshly prepared brain homogenate, previously equilibrated at 37 °C in a water bath for 5 min, 400 μL of (2×10^{-1} mmol) methanolic solution of freshly prepared MEPCDSs **10c**, **14** and **19b** was added, the prepared mixture was kept at 37 °C all the time of the experiment. Samples of 0.5 mL were withdrawn from the mixture at different time intervals (1, 2, 4, 8, 16, 32, and 64 min) and immediately added to 3 mL of ice-cooled methanol, vortexes, and places in a deep freezer (−80 °C). When all the samples have been collected, they were centrifuged, and the supernatants were filtered through nitrocellulose membrane filter (0.22 μm) and analyzed by HPLC for their contents of the MEPCDSs **10c**, **14** and **19b** and their corresponding $MEPQ^+$s derivatives. The apparent pseudo first order rate constant of appearance ($K_{disapp.}$, min^{-1}) of the MEPCDS was determined by linear regression of the Ln of the MEPCDS peak area against time in minutes.

3.2.3. In vivo distribution studies

Four groups, each of three Sprague-Dawley male rats of average weight of 120–150 g were anesthetized with 0.7 mL solution of 25% urethane in water. A freshly prepared solution of MEPCDSs **10c** or **14** in DMF (25 mg/mL) was injected through the jugular vein in a dose level of 20 mg/kg of animal body weight. At appropriate time intervals (10, 20, and 45 min), 1 mL of blood was withdrawn and added immediately to a tarred tube containing 4 mL of acetonitrile, which was afterwards weighed to determine the amount of the blood added. The samples kept freezing (−80 °C) until analysis. The animal was then decapitated, and the brain was collected, weighed and immediately kept in a deep freezer (−80 °C). The whole brain homogenized in 1 mL of water, 4 mL of 5% DMF in acetonitrile was added to the homogenate, and the mixture was homogenized again and centrifuged at 4000 rpm for 10 min. Blood samples were mixed with 4 mL of acetonitrile, for protein precipitation, and vortexes at 4000 rpm for 10 min. The supernatants from the brain and the blood samples were filtered through nitrocellulose membrane filter (0.22 μm) and analyzed by HPLC. The amount of the quaternary derivatives was determined from the HPLC spectrum in relation to a recovery experiment made by adding a specific amount of the $MEPQ^+$s **9c** or **13** to a blank rat brain and blood and treated under the same manner.

3.2.4. Antidepressant screening using tail suspension technique

Adult male albino Swiss-Webster mice (22 ± 2 g) were obtained from the animal house, Cairo. The mice were housed in a quiet and temperature and humidity-controlled room (22 ± 3 °C and 60 ± 5%, respectively) in which a 12 h light/dark cycle was maintained (08:00–20.00 h light). The animals were acclimated to their environment for at least 2 days before the experiments and were allowed free access to food and water before being tested.

On the testing day, mice were assigned into different groups ($n = 6$ for each group). The tested compounds and reference drug (imipramine) were dissolved in carboxymethylcellulose (CMC) solution (0.5% w/v in water). The prepared MEPCDSs **10a**, **10c**, **14** and **19a** and their corresponding quaternary $MEPQ^+$ **9a**, **9c**, **13** and **18a** (10 mg/kg) and imipramine (10 mg/kg) were injected ip to mice at a volume of 0.5 mL per 100 g body weight. Control animals were similarly treated with CMC solution (0.5% w/v in water). One hour later, the mice were suspended by the tail to the edge of a shelf 80 cm above the floor. The tail was secured to the shelf by adhesive tape placed approximately 1cm from the tip of the tail. The duration of the immobility was recorded for a period of 6 min. Mice were considered immobile only when they hung passively and completely motionless.

Acknowledgment

Authors introduce their great thanks to Dr. Al-Shimaa Faisel, Pharmacology Department, Faculty of Pharmacy, Minia University for her valuable help in measuring the antidepressant activity.

References and notes

1. Rapoport, S. In *Blood–Brain Barrier in Physiology and Medicine*; Rapoport, S., Ed.; Raven Press: New York, 1976. pp 43–86.
2. Chem, P.; Bodor, N.; Wu, W.; Prokai, L. *J. Med. Chem.* **1998**, *41*, 3773.
3. Rana, K.; Bodor, N.; Elkoussi, A.; Raad, I.; Miyake, A.; Houck, H.; Gilder-Sleeve, N. *J. Med. Virol.* **1986**, *20*, 1.
4. Anderson, W.; Simpkins, J.; Woodard, P.; Winood, D.; Stern, W.; Bodor, N. *Psychopharmacology (Berl.)* **1987**, *92*, 157.
5. Greig, N.; Daly, E.; Sweeney, D.; Rapoport, S. *Cancer Chemother. Pharmacol.* **1990**, *25*, 320.
6. Krogsgaard-Larsen, P.; Christiansen, A. *Eur. J. Med. Chem.* **1979**, *14*, 157.
7. Brewster, M.; Raghavan, K.; Pop, E.; Bodor, N. *Antimicrob. Agents Chemother.* **1994**, *38*, 817.
8. Pop, E.; Bodor, N. *Review-Epilepsy Res.* **1992**, *13*, 1.
9. Raghavan, K.; Loftsson, T.; Brewster, M.; Bodor, N. *Pharm. Res.* **1992**, *9*, 743.
10. Brewster, M.; Pop, E.; Braunstein, A.; Pop, A.; Druzgala, A.; Drinculescu, A.; Anderson, W.; Elkoussi, A.; Bodor, N. *Pharm. Res.* **1993**, *10*, 1356.
11. Brewster, M.; Bartruff, M.; Anderson, W.; Druzgala, P.; Bodor, N.; Pop, E. *J. Med. Chem.* **1994**, *37*, 4237.
12. Eisner, U.; Kuthan, J. *Chem. Rev.* **1972**, *72*, 1.
13. Bodor, N.; Farrag, H.; Omar, F. *Pharm. Sci.* **1995**, *1*, 301.
14. Bodor, N.; Farag, H.; Brewster, M. *Science* **1981**, *214*, 1370.
15. Bodor, N.; Farag, H. *J. Med. Chem.* **1983**, *26*, 313.
16. Pop, E.; Loftsson, T.; Bodor, N. *Pharm. Res.* **1991**, *8*, 1044.
17. Bodor, N.; Farrag, H.; Omar, F. *Bull. Pharm. Sci.* **1993**, *16*, 175. Assiut University.
18. Mai, A.; Artico, M.; Esposito, M.; Ragno, R.; Sbardella, G.; Massa, S. *Farmaco* **2003**, *58*, 231.
19. Kuyl-Yeheskiely, E.; Tromp, C. M.; Van der Marel, G. A.; Boom, J. H. V. *Tetrahedron Lett.* **1987**, *28*, 4461.
20. Solomons, T. W. G. In *Solomons Organic Chemistry*; Magida, S., Ed., 6th ed.; John Wiley & Sons: New York, 1996. pp 833–834.
21. Francis, A.; Sundberg, J. In *Advanced Organic Chemistry Part B: Reactions and Synthesis*, 5th ed.; Springer Sceince + Business media: Virginia, 2007. pp 1008–1010.
22. Xu, Y.-J.; Zhao, S.; Bi, S. *Acta Crystallogr., Sect. E* **2007**, *63*, o4633.
23. Lin, M.; Liu, S.-X. *Acta Crystallogr., Sect. E* **2007**, *63*, o3974.
24. Sinha, N.; Jain, S.; Tilekar, A.; Upadhayaya, R. S.; Kishore, N.; Jana, G. H.; Arora, S. K. *Bioorg. Med. Chem. Lett.* **2005**, *15*, 1573.
25. Shi, X.-F.; He, L.; Ma, G.-Z.; Yuan, C.-C. *Acta Crystallogr., Sect. E* **2007**, *63*, o1119.
26. Yang, D.-S. *J. Chem. Crystallogr.* **2007**, *37*, 343.
27. Fryer, R.; Earley, J.; Schneider, J.; Sternbach, L. *Org. Chem.* **1970**, *35*, 2455.
28. Khan, K. M.; Rasheed, M.; Zia, U.; Hayat, S.; Kaukab, F.; Choudhary, M. I.; Atta ur, R.; Perveen, S. *Bioorg. Med. Chem.* **2003**, *11*, 1381.
29. Melnyk, P.; Leroux, V.; Sergheraert, C.; Grellier, P. *Bioorg. Med. Chem. Lett.* **2006**, *16*, 31.
30. Fun, H.-K.; Sivakumar, K.; Lu, Z.-L.; Duan, C.-Y.; Tian, Y.-P.; You, X.-Z. *Acta Crystallogr., Sect. C* **1996**, *52*, 986.
31. Powell, M. F.; Wu, J. C.; Bruice, T. C. *Am. Chem. Soc.* **1984**, *106*, 3850.
32. Brewster, M. E.; Kaminski, J.; Gabanyi, Z.; Czako, K.; Simay, A.; Bodor, N. *Tetrahedron* **1989**, *45*, 4395.
33. Bodor, N.; El-Kommos, M. E. *Bull. Pharm. Sci.* **1986**, *9*, 14. Assiut University.
34. Woodard, P. A.; Winwood, D.; Brewster, M. E.; Estes, K. S.; Bodor, N. *Drug Des. Delivery* **1990**, *6*, 15.
35. Rahimy, M. H.; Simpkins, J. W.; Bodor, N. In *Trends in Medicinal Chemistry*; Sarel, S., Mechoulam, R., Agranat, I., Eds.; Blackwell Scientific: New York, 1992. pp 369–376.
36. Sheha, M.; Al-Tayeb, A.; El-Sherief, H.; Farag, H. *Bioorg. Med. Chem.* **2003**, *11*, 1865.

37. Xu, Q.; Pan, Y.; Yi, L. T.; Li, Y. C.; Mo, S. F.; Jiang, F. X.; Qiao, C. F.; Xu, H. X.; Lu, X. B.; Kong, L. D.; Kung, H. F. *Biol. Pharm. Bull.* **2008**, *31*, 1109.
38. Sakakibara, H.; Yoshino, S.; Kawai, Y.; Terao, J. *Biosci. Biotechnol. Biochem.* **2008**, *72*, 94.
39. Bhattamisra, S. K.; Khanna, V. K.; Agrawal, A. K.; Singh, P. N.; Singh, S. K. *J. Ethnopharmacol.* **2008**, *117*, 51.
40. Wei, X. H.; Cheng, X. M.; Shen, J. S.; Wang, Z. T. *J. Ethnopharmacol.* **2008**, *117*, 339.
41. Schroeder, F. A.; Lin, C. L.; Crusio, W. E.; Akbarian, S. *Biol. Psychiat.* **2007**, *62*, 55.
42. Mineur, Y. S.; Picciotto, M. R.; Sanacora, G. *Biol. Psychiat.* **2007**, *61*, 250.
43. Liu, X.; Stancliffe, D.; Lee, S.; Mathur, S.; Gershenfeld, H. K. *Biol. Psychiat.* **2007**, *62*, 81.